# Supplementary Information

## Nanoplasmonic Quantification of Tumor-derived Extracellular Vesicles in Plasma Microsamples for Diagnosis and Treatment Monitoring

Kai Liang[1, 2†], Fei Liu[1†], Jia Fan[1], Dali Sun[1], Chang Liu[3], Christopher J. Lyon[1], David W. Bernard[4], Yan Li[2], Kenji Yokoi[1], Matthew H. Katz[5], Eugene J. Koay[6], Zhen Zhao[7], Ye Hu[3*]

**Affiliations**

[1]Department of Nanomedicine, Houston Methodist Research Institute, 6670 Bertner Avenue, Houston, Texas 77030, USA.

[2]Institute of Biophysics, Chinese Academy of Sciences, 15 Datum Road, Chaoyang District, Beijing 100101, China.

[3]School of Biological and Health Systems Engineering, Virginia G. Piper Biodesign Center for Personalized Diagnostics, The Biodesign Institute, Arizona State University, 1001 S. McAllister Ave. B 130-B, Tempe, AZ 85287, USA.

[4]Department of Pathology and Genomic Medicine, Houston Methodist Hospital, 6565 Fannin St, Houston, Texas 77030, USA.

[5]Department of Surgical Oncology, Division of Surgery, The University of Texas MD Anderson Cancer Center, 1515 Holcombe Blvd, Houston, Texas 77030, USA.

[6]Division of Radiation Oncology, University of Texas M.D. Anderson Cancer Center, 1515 Holcombe Blvd, Houston, Texas 77030, USA.

[7]Department of Laboratory Medicine, Clinical Center, National Institutes of Health, 10 Center Drive, Building 10, Bethesda, MD 20892, USA.

[†] Kai Liang and Fei Liu contributed equally to the work.

[*] Correspondence should be addressed to Y.H. (tyhu@asu.edu)

Table of Contents

## Supplementary Methods

**Preparation of EV-free plasma samples.** Plasma samples were centrifuged at 110,000 g overnight, and supernatants were collected as EV-free plasma, and analyzed by Western blot analysis, which found that the EV marker proteins CD63 and Tsg101 were markedly depleted in EV-free plasma supernatants, but highly enriched in the matching plasma precipitates (Fig. S3c and S3d)

**Selection of the pixel intensity threshold for the procession of DFM images.** NIH IMAGE J image analysis software was used to analyze DFM images. DFM AuS-EV-AuS signal was quantified using a pixel intensity threshold of 255 to exclude AuS-EV signal detected at lower thresholds (Fig. S13), since this cut-off was found to detect < 0.4 % of AuS-EV spots and 0 % of AuR-EV spots in 20 EV wells incubated with both AuS and AuR probe, where false positive AuS-EV signal accounting for ≤ 0.2 % of the total AuS-EV-AuR signal.

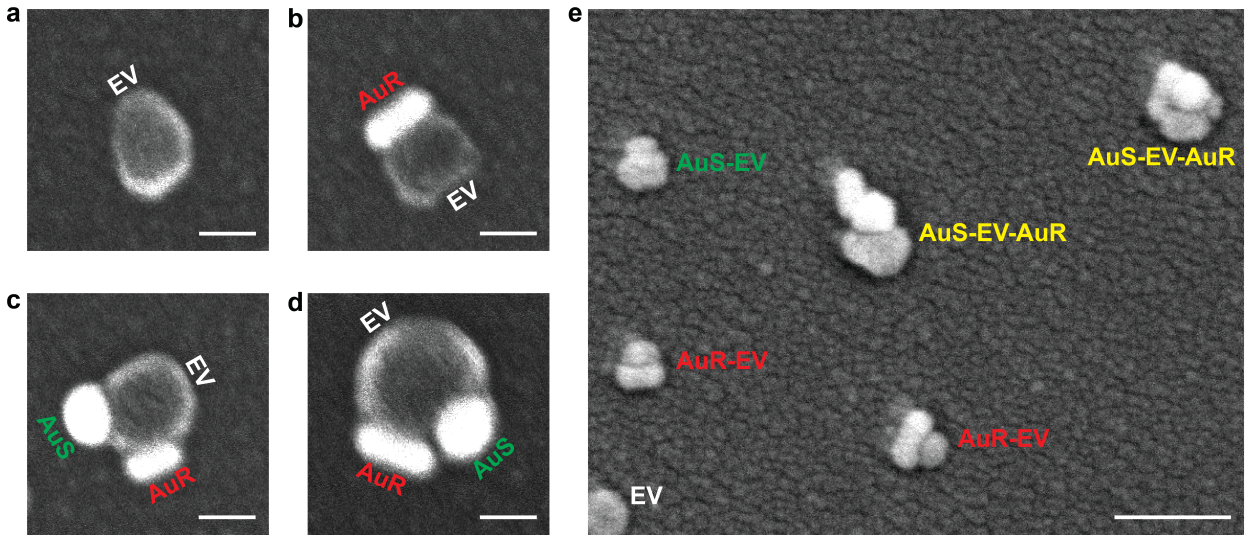


**Figure S1.** SEM images of (a) bare EV captured on the sensor chip, (b) EV binding with one AuR GNP and (c -d) EVs binding with both AuR and AuS GNPs, and (e) EV dispersion on the assay chip. Scale bar: (a-d) 50 nm and (e) 250 nm.

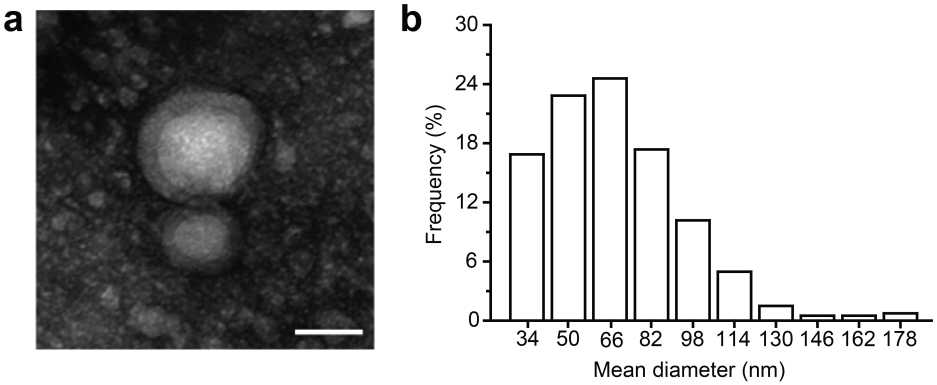


**Figure S2.** (a) TEM image and (b) dynamic light scattering (DLS)-determined size distribution of purified human plasma EVs. Scale bar: 20 nm.

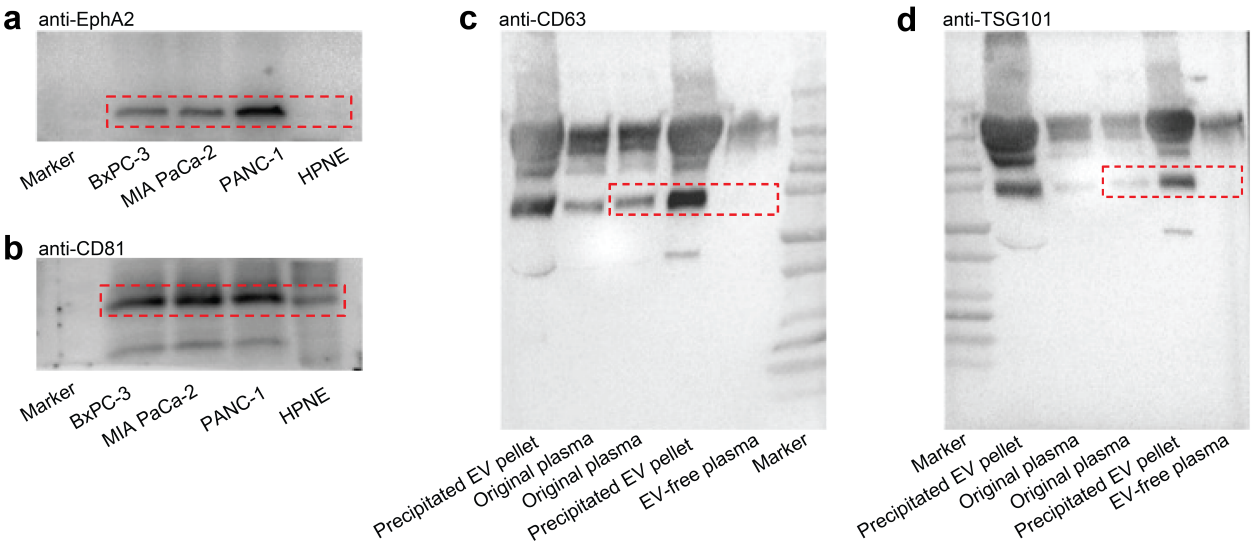


**Figure S3.** Complete images of Western blot analyses for EVs isolated from (a-b) human pancreatic cell lines (Figure 3) or (c-d) human plasma after hybridization with (a) anti-EphA2, (b) anti-CD81, (c) anti-CD63 or (d) anti-TSG101. The same amount of BCA-quantified protein extract was loaded in all wells. Data shown in (a) and (b) represent different regions of the same blot that were cut and then separately hybridized with the indicated antibodies. Extra bands detected in (c) and (d) represent blocking artifacts from high abundance plasma and marker proteins. All wells were loaded with 10 µg BCA-quantified protein extract. Target protein bands are labeled by dashed boxes.

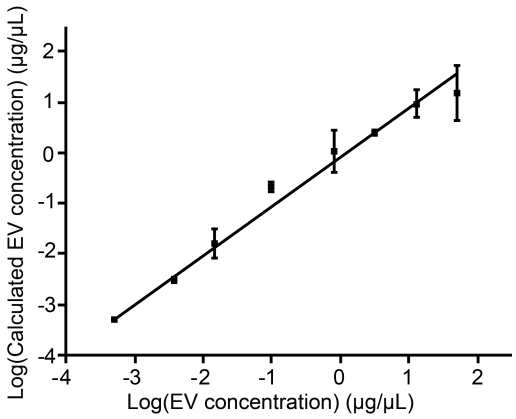


**Figure S4.** Linear range of the log (nPES-calculated EV concentration) *vs*. log (known EV concentration) in EV-spiked standard samples (5E-4, 3.75E-3, 1.5E-2, 0.1, 0.8, 3.2, 12.8, 51.2 µg/µL). A strong correlation ($r^2$ = 0.99) was obtained in this concentration range. Data represent mean ± SEM; n = 3 replicates/sample.

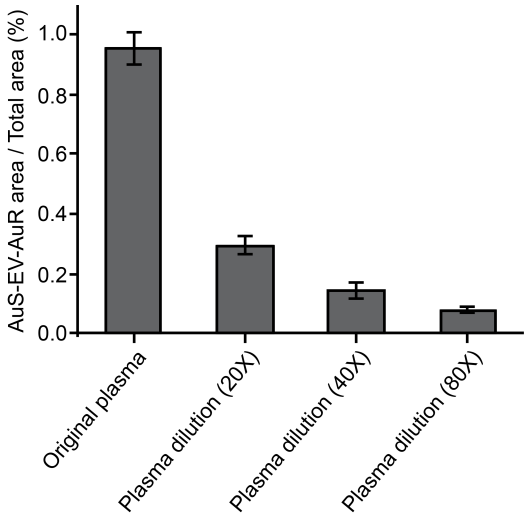


**Figure S5.** Representative nPES signal in undiluted human plasma (> 50 μg/μL nPES assay upper limit) and successive PBS dilutions. Data represent mean ± SEM; n = 3 replicates/sample.

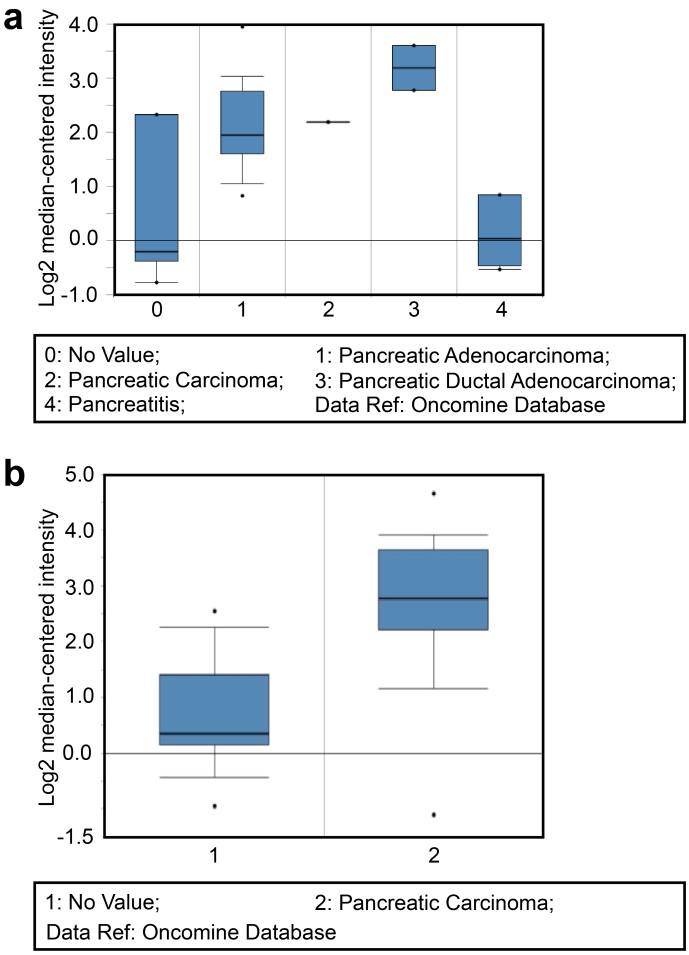


**Figure S6.** EphA2 expression levels in two Oncomine datasets comparing gene expression in (a)[1] normal human pancreas (No value; n = 5), pancreatic cancer (pancreatic adenocarcinoma, n = 14; pancreatic carcinoma, n = 1; pancreatic ductal adenocarcinoma, n = 2) and Pancreatitis (n=5) tissue samples and (b)[2] normal human pancreas (No value; n = 16) and pancreatic carcinoma (sample number, n = 36) tissue samples. The "No Value" label indicates normal samples not assigned a cancer designation. Boxes span the interquartile range, the line within boxes represent the median, and whiskers indicate the minimum and maximum values.

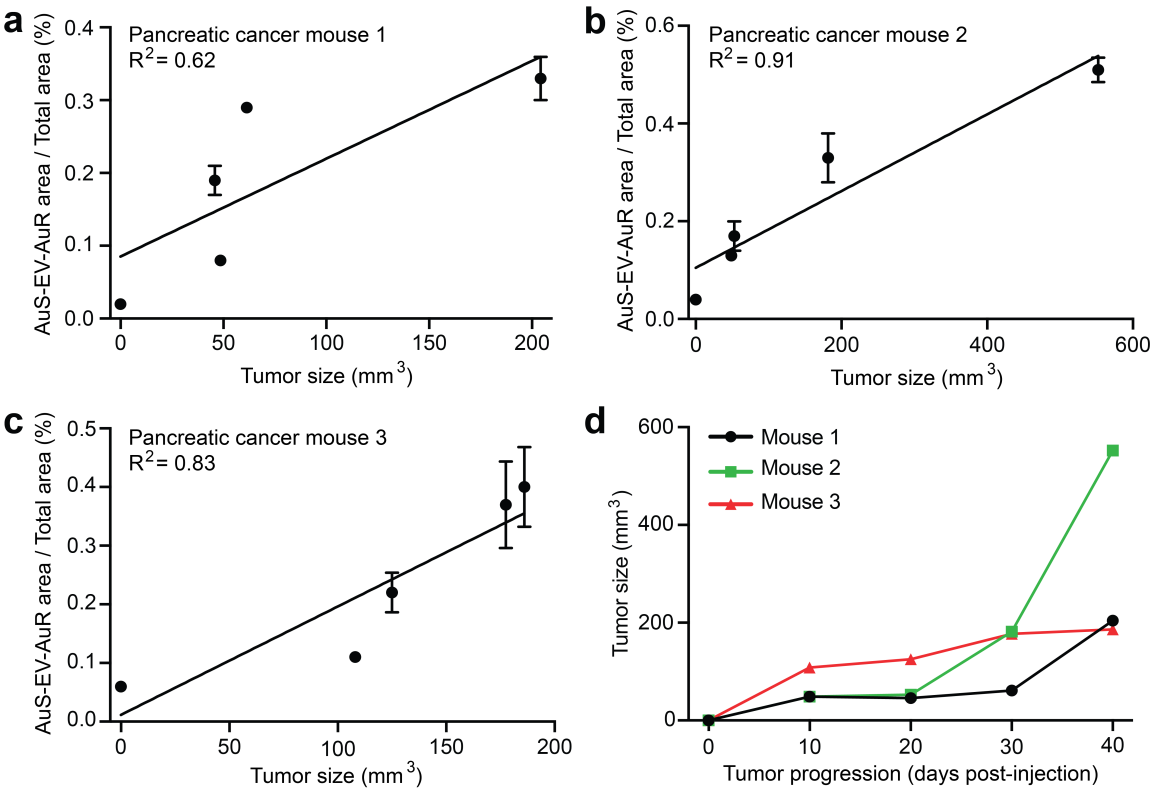


**Figure S7**. Correlation of pancreatic tumor size with (a-c) nPES signal and (d) time post-injection in nude mice subcutaneously injected with $2 \times 10^6$ with PANC-1 pancreatic tumor cells.

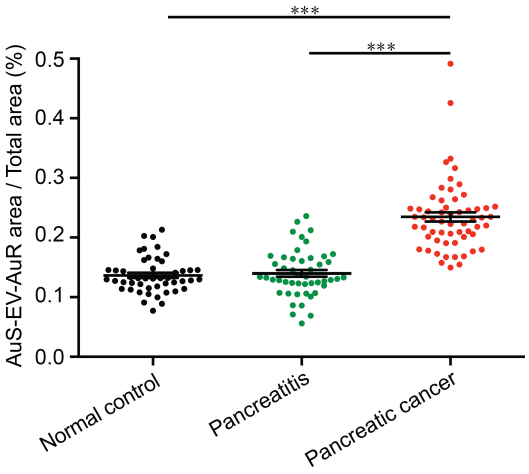


**Figure S8.** Comparison of EphA2-EV levels in plasma samples from normal control (n = 48), chronic pancreatitis (n = 48) and pancreatic cancer (n = 59) patients, with 1 μL unprocessed plasma. Data represent mean ± SEM. ***, $p < 0.001$ by one-way ANOVA.

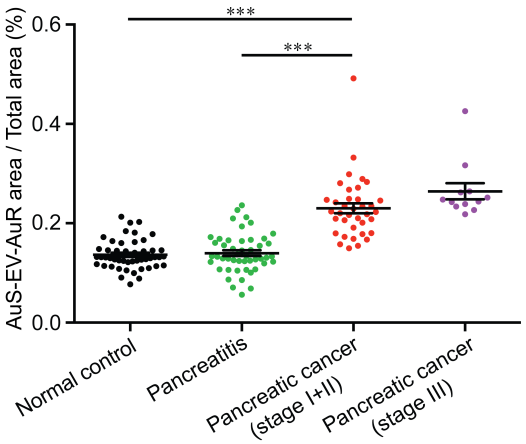


**Figure S9.** Comparison of EphA2-EV levels in plasma samples from normal control (n = 48), pancreatitis (n = 48) and stage I + II (S1 + S2; n = 37) and III (S3; n = 12) pancreatic cancer patients. Note that 10 pancreatic cancer patients did not have recorded tumor stage data. Data represent mean ± SEM. ***, $p < 0.001$ by one-way ANOVA.

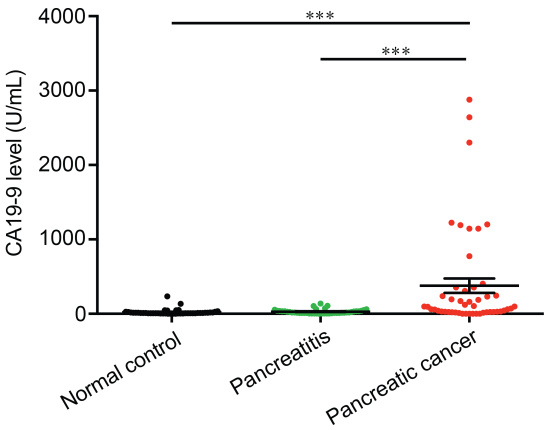


**Figure S10.** Comparison of CA19-9 levels in plasma samples from normal control (n = 44), pancreatitis (n = 43) and pancreatic cancer patients (n = 49). Note that some patients did not have recorded CA19-9 data due to insufficient sample. Data represent mean ± SEM; ***, $p < 0.001$ by Kruskal-Wallis one-way ANOVA.

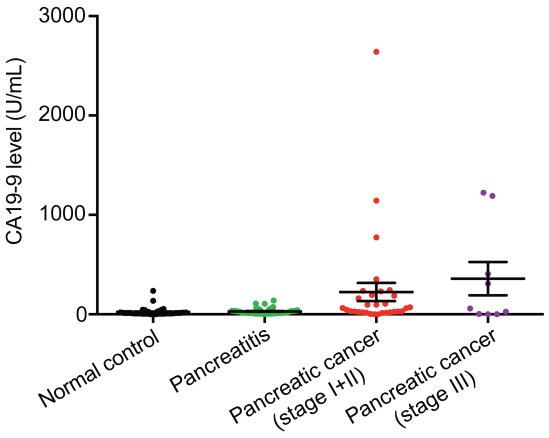


**Figure S11.** Comparison of CA19-9 levels in plasma samples from normal control (n = 44), pancreatitis (n = 43) and stage I + II (S1 + S2; n = 31) and III (S3; n = 9) pancreatic cancer patients. Note that some patients did not have recorded CA19-9 data due to insufficient sample. Data represent mean ± SEM. Kruskal-Wallis one-way ANOVA was used for data comparison.

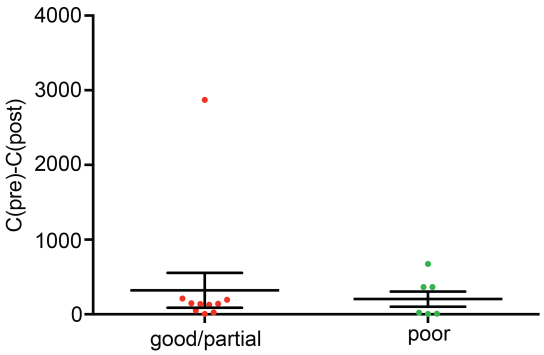


**Figure S12.** Difference in plasma CA19-9 levels before (C(pre)) and after (C(post)) therapy in patients with good/partial (< 50 % viable tumor cells, n = 13) and poor (> 50 % viable tumor cells, n = 10) responses to therapy. Data represent mean ± SEM. Student t-test was used for data comparison.

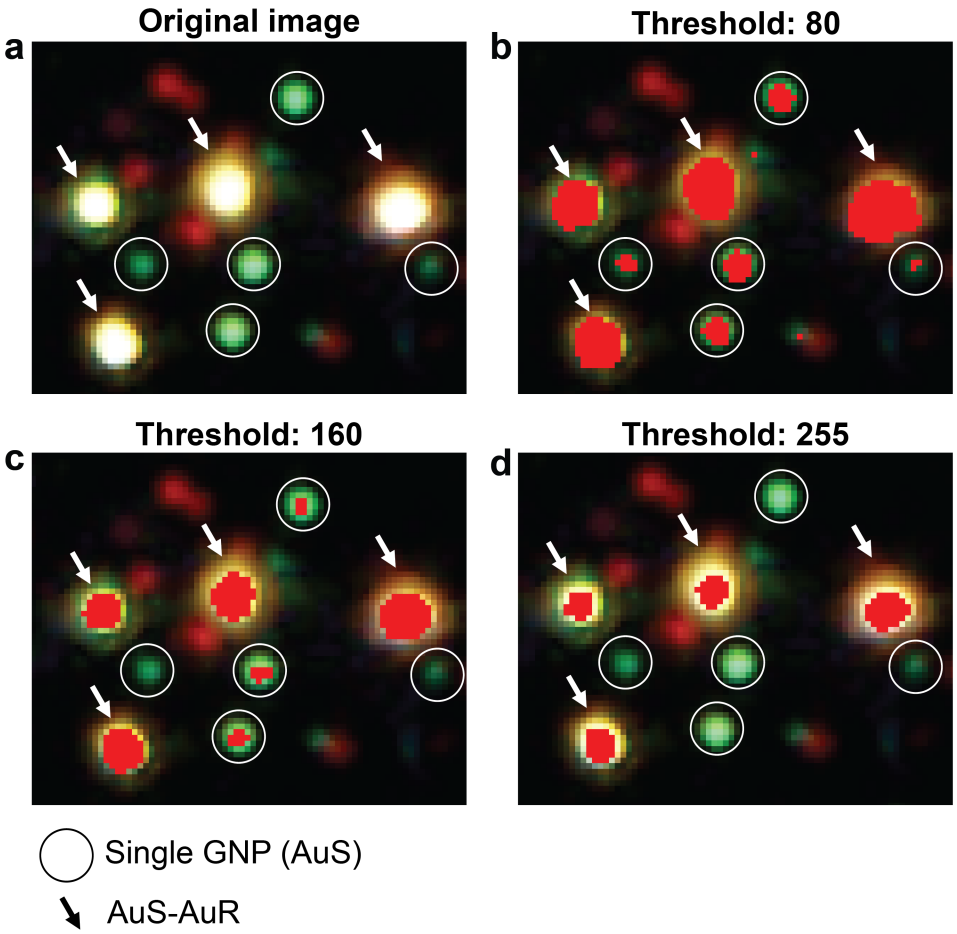


**Figure S13.** Image of nPES signal detected (a) without a software threshold and "AuS-EV-AuR" signal recognized after intensity thresholds of (b) 80, (c) 160 and (d) 255 are applied to the image, with detected signal indicated by intense red pixel maps. Circles indicate AuS-EV signal and arrow mark true AuS-EV-AuR signal. Note that AuR-EV (dim red) spots were not recognized at these thresholds.

**Table S1**. Reproducibility of nPES results with different input plasma volumes.

| Volume | Mean | CV % |
|---|---|---|
| 0.5 µL | 0.779 | 13.5 % |
| 1.0 µL | 0.712 | 3.81 % |
| 2.0 µL | 0.704 | 3.04 % |
| 5.0 µL | 0.706 | 2.86 % |

**Table S2**. Repeatability of EphA2 EV nPES results in two selected plasma samples with low and high nPES signals, subsequently found to be from patients with stage II (patient 1) and stage III (patient 2) pancreatic cancer. Samples were analyzed with 20 replicates per day over 3 days to generate 60 values per sample.

| | Within-day mean | Between-day mean | Within-day CV % | Between-day CV % |
|---|---|---|---|---|
| Patient 1 | 0.160 | 0.162 | 9.14 % | 9.70 % |
| Patient 2 | 0.311 | 0.310 | 4.93 % | 6.99 % |

**Table S3.** Membrane proteins identified by proteomic analysis of EVs from the human pancreatic cancer cell lines PANC-1, MIA PaCa-2, and BXPC-3. The 26 proteins that were expressed in at least 2 cell lines (highlight with gray) were then analyzed in ONCOMINE database, to compare gene expression level of each protein in pancreatic cancer, NC, and chronic Pancreatitis tissue samples.

| | Membrane Proteins Identified | BxPC-3 cell | MIA cell | PANC-1 cell | SUM |
|---|---|---|---|---|---|
| 1 | CD81 antigen | √ | √ | √ | 3 |
| 2 | CD9 antigen | √ | √ | √ | 3 |
| 3 | Ephrin type-A receptor 2 | √ | √ | √ | 3 |
| 4 | Integrin alpha-3 | √ | √ | √ | 3 |
| 5 | Integrin alpha-V | √ | √ | √ | 3 |
| 6 | Intercellular adhesion molecule 1 | √ | √ | √ | 3 |
| 7 | Ras-related protein Ral-A | √ | √ | √ | 3 |
| 8 | Aldehyde dehydrogenase family 16 member A1 | √ | √ | | 2 |
| 9 | CD63 antigen | | √ | √ | 2 |
| 10 | DnaJ homolog subfamily C member 13 | √ | | √ | 2 |
| 11 | Epithelial cell adhesion molecule | √ | | √ | 2 |
| 12 | Guanine nucleotide-binding protein G(I)/G(S)/G(T) subunit beta-1 | | √ | √ | 2 |
| 13 | Integrin alpha-6 | | √ | √ | 2 |
| 14 | Immunoglobulin superfamily member 8 | √ | √ | | 2 |
| 15 | Integrin beta-4 | √ | | √ | 2 |
| 16 | Integrin beta-5 | | √ | √ | 2 |
| 17 | Isoform 2 of G-protein coupled receptor 126 | √ | | √ | 2 |
| 18 | Keratin, type I cytoskeletal 19 | √ | | √ | 2 |
| 19 | Plasma membrane calcium-transporting ATPase 4 | | √ | √ | 2 |
| 20 | Plexin-B2 | √ | | √ | 2 |
| 21 | Protein tweety homolog 3 | | √ | √ | 2 |
| 22 | Secretory carrier-associated membrane protein 3 | √ | | √ | 2 |
| 23 | Sodium/potassium-transporting ATPase subunit beta-3 (Fragment) | √ | | √ | 2 |
| 24 | Sushi domain-containing protein 2 | | √ | √ | 2 |
| 25 | Tetraspanin-14 | √ | √ | | 2 |
| 26 | Transgelin-2 | | √ | √ | 2 |
| 27 | Adenylyl cyclase-associated protein 1 | | | √ | 1 |
| 28 | Adenylyl cyclase-associated protein 2 | | | √ | 1 |
| 29 | Alkaline phosphatase, placental-like | | | √ | 1 |
| 30 | Alpha-1,3-mannosyl-glycoprotein 4-beta-N-acetylglucosaminyltransferase B (Fragment) | | | √ | 1 |
| 31 | Amiloride-sensitive sodium channel subunit alpha | | | √ | 1 |
| 32 | Annexin A13 | | | √ | 1 |
| 33 | AP-2 complex subunit mu (Fragment) | | | √ | 1 |
| 34 | Basigin (Fragment) | | √ | | 1 |
| 35 | BRO1 domain-containing protein BROX | √ | | | 1 |
| 36 | BTB/POZ domain-containing protein KCTD16 | √ | | | 1 |
| 37 | Cadherin-18 (Fragment) | √ | | | 1 |
| 38 | Calcium permeable stress-gated cation channel 1 | √ | | | 1 |
| 39 | CD70 antigen | | | √ | 1 |
| 40 | CD99 antigen-like protein 2 | | | √ | 1 |
| 41 | Class I histocompatibility antigen, Gogo-A*0101 alpha chain | | √ | | 1 |
| 42 | Class I histocompatibility antigen, Gogo-OKO alpha chain | | | √ | 1 |
| 43 | Clathrin light chain A | | √ | | 1 |
| 44 | Claudin-7 | √ | | | 1 |
| 45 | Complement receptor type 2 | | | √ | 1 |
| 46 | Contactin-6 | | | √ | 1 |
| 47 | C-type mannose receptor 2 | | | √ | 1 |
| 48 | Desmoglein-2 | √ | | | 1 |
| 49 | DnaJ homolog subfamily A member 1 | √ | | | 1 |
| 50 | EH domain-binding protein 1-like protein 1 | | | √ | 1 |
| 51 | Embigin | | | √ | 1 |
| 52 | Ephrin type-B receptor 4 | | | √ | 1 |
| 53 | Equilibrative nucleoside transporter 1 | | | √ | 1 |
| 54 | Fermitin family homolog 3 | √ | | | 1 |
| 55 | G protein-regulated inducer of neurite outgrowth 1 | | √ | | 1 |
| 56 | General receptor for phosphoinositides 1-associated scaffold protein (Fragment) | √ | | | 1 |
| 57 | G-protein coupled receptor 126 | | √ | | 1 |
| 58 | Guanine nucleotide-binding protein G(I)/G(S)/G(O) subunit gamma-12 | √ | | | 1 |
| 59 | Guanine nucleotide-binding protein G(s) subunit alpha | | √ | | 1 |
| 60 | Guanine nucleotide-binding protein G(s) subunit alpha isoforms short (Fragment) | √ | | | 1 |
| 61 | High affinity cationic amino acid transporter 1 | | √ | | 1 |
| 62 | IgG receptor FcRn large subunit p51 (Fragment) | √ | | | 1 |
| 63 | Inactive tyrosine-protein kinase 7 | | | √ | 1 |
| 64 | Interferon-induced transmembrane protein 1 | | √ | | 1 |
| 65 | Isoform 2 of BRO1 domain-containing protein BROX | | | √ | 1 |
| 66 | Isoform 2 of CD97 antigen | | | √ | 1 |
| 67 | Isoform 2 of Guanine nucleotide-binding protein G(I)/G(S)/G(T) subunit beta-1 | √ | | | 1 |
| 68 | Isoform 2 of Metal transporter CNNM3 | | | √ | 1 |
| 69 | Isoform 2 of Sodium/potassium-transporting ATPase subunit beta-1 | | | √ | 1 |
| 70 | Isoform 2 of Syntaxin-7 | | | √ | 1 |
| 71 | Isoform 2 of Vang-like protein 1 | √ | | | 1 |
| 72 | Isoform 3 of Choline transporter-like protein 1 | √ | | | 1 |
| 73 | Isoform 3 of Choline transporter-like protein 2 | | | √ | 1 |
| 74 | Isoform 3 of Protein tweety homolog 3 | √ | | | 1 |
| 75 | Isoform 3 of Receptor-type tyrosine-protein phosphatase U | | | √ | 1 |

| | | | | | |
|---|---|---|---|---|---|
| 76 | Isoform 4 of Thyroid adenoma-associated protein | | | √ | 1 |
| 77 | Isoform Alpha of Nectin-2 | | | √ | 1 |
| 78 | Isoform Alpha-2 of Guanine nucleotide-binding protein G(o) subunit alpha | | | √ | 1 |
| 79 | Isoform Non-brain of Clathrin light chain B | √ | | | 1 |
| 80 | Kin of IRRE-like protein 1 | | | √ | 1 |
| 81 | Latent-transforming growth factor beta-binding protein 2 | | | √ | 1 |
| 82 | Leucine-rich repeat-containing protein 8A | √ | | | 1 |
| 83 | Lipolysis-stimulated lipoprotein receptor | | | √ | 1 |
| 84 | Lipoxygenase homology domain-containing protein 1 | √ | | | 1 |
| 85 | Membrane-associated progesterone receptor component 2 | | | √ | 1 |
| 86 | Monocarboxylate transporter 2 | √ | | | 1 |
| 87 | Myelin protein zero-like protein 1 | | √ | | 1 |
| 88 | Na(+)/H(+) exchange regulatory cofactor NHE-RF1 (Fragment) | √ | | | 1 |
| 89 | Na(+)/H(+) exchange regulatory cofactor NHE-RF2 (Fragment) | √ | | | 1 |
| 90 | Neural cell adhesion molecule L1 | | | √ | 1 |
| 91 | Patr class I histocompatibility antigen, A-2 alpha chain | √ | | | 1 |
| 92 | Phosphatidylinositol-glycan biosynthesis class X protein | | | √ | 1 |
| 93 | Phosphorylase b kinase regulatory subunit beta | | √ | | 1 |
| 94 | Plexin-A4 | √ | | | 1 |
| 95 | Prominin-2 | √ | | | 1 |
| 96 | Protein eva-1 homolog B | | | √ | 1 |
| 97 | Protein ITFG3 | | √ | | 1 |
| 98 | Protein S100-A10 | | | √ | 1 |
| 99 | Putative HLA class I histocompatibility antigen, alpha chain H | | √ | | 1 |
| 100 | Ragulator complex protein LAMTOR1 (Fragment) | | | √ | 1 |
| 101 | Ras-related C3 botulinum toxin substrate 3 (Fragment) | √ | | | 1 |
| 102 | Ras-related protein Ral-B | √ | | | 1 |
| 103 | Ras-related protein Rap-1b | | | √ | 1 |
| 104 | Receptor-type tyrosine-protein phosphatase alpha | | √ | | 1 |
| 105 | Receptor-type tyrosine-protein phosphatase kappa | √ | | | 1 |
| 106 | Regulating synaptic membrane exocytosis protein 1 | | | √ | 1 |
| 107 | Reversion-inducing cysteine-rich protein with Kazal motifs | | | √ | 1 |
| 108 | RT1 class I histocompatibility antigen, AA alpha chain | | √ | | 1 |
| 109 | Serine/threonine-protein kinase RIO2 | | | √ | 1 |
| 110 | Sodium- and chloride-dependent creatine transporter 1 (Fragment) | √ | | | 1 |
| 111 | Sodium/potassium-transporting ATPase subunit beta-1 | | √ | | 1 |
| 112 | Sulfate transporter | | | √ | 1 |
| 113 | Synaptic vesicle membrane protein VAT-1 homolog (Fragment) | | | √ | 1 |
| 114 | Tetraspanin-15 (Fragment) | | | √ | 1 |
| 115 | Tetraspanin-3 | √ | | | 1 |
| 116 | Tetraspanin-31 | √ | | | 1 |
| 117 | Tetraspanin-4 | | √ | | 1 |
| 118 | Tetraspanin-4 (Fragment) | | | √ | 1 |
| 119 | Tetraspanin-9 | √ | | | 1 |
| 120 | Thrombomodulin | √ | | | 1 |
| 121 | Transgelin-2 (Fragment) | √ | | | 1 |
| 122 | Transmembrane 4 L6 family member 18 | | | √ | 1 |
| 123 | Transmembrane emp24 domain-containing protein 10 | | | √ | 1 |
| 124 | Transmembrane protein 246 | | | √ | 1 |
| 125 | Tumor necrosis factor receptor superfamily member 10D | √ | | | 1 |
| 126 | Type I inositol 1,4,5-trisphosphate 5-phosphatase (Fragment) | | | √ | 1 |
| 127 | Tyrosine-protein kinase receptor | | | √ | 1 |
| 128 | Vesicle-associated membrane protein 2 | | √ | | 1 |

**Table S4**. Estimated Total-EV and EphA2-EV concentrations in pooled patient plasma samples.

| Plasma sample | Total-EVs / µL plasma[a] | Total-EVs /assay well (5 µL @ 40X dil.) | Total-EVs protein (ng/µL)[b] | EphA2-EVs protein (ng/µL)[c] | EphA2-EVs / Total-EVs plasma (%)[d] | EphA2-EVs / assay well[e] |
|---|---|---|---|---|---|---|
| Pancreatic cancer | $9.1\times10^{9}$ | $1.14\times10^{9}$ | 2006 | 119 | 5.93 | $6.75\times10^{8}$ |
| Pancreatitis | $8.7\times10^{9}$ | $1.09\times10^{9}$ | 2196 | 5.73 | 0.26 | $2.26\times10^{8}$ |
| Normal control | $7.3\times10^{9}$ | $0.91\times10^{9}$ | 2316 | 3.56 | 0.15 | $1.10\times10^{7}$ |

[a] Nanosight-generated EV counts;
[b] BCA protein quantitation of ExoQuick-isolated plasma EVs
[c] Calculated with nPES assay data and the standard curves equation
[d] EphA2-EV to Total-EV protein ratio
[e] EphA2-EVs/Total-EVs x Total-EVs/assay well

**Table S5.** Demographics of normal control, pancreatitis, stage I + II pancreatic cancer, stage III pancreatic cancer and all pancreatic cancer patients. Note that 10 pancreatic cancer patients did not have recorded tumor stage data.

| | Normal control *vs.* Pancreatitis *vs.* Pancreatic cancer | | | | |
|---|---|---|---|---|---|
| | Normal control | Pancreatitis | Pancreatic cancer stage (I+II) | Pancreatic cancer stage (III) | Pancreatic cancer (stage I-III) |
| Sex (No. of Patients) | | | | | |
| Men No. (%) | 19 (39.6) | 25 (52.1) | 22 (59.5) | 7 (58.3) | 33 (55.9) |
| Women No. (%) | 29 (60.4) | 23 (47.9) | 15 (40.5) | 5 (41.7) | 26 (44.1) |
| Age median (range) year | 61.9 (19-89) | 52.3 (27-78) | 67.2 (46-85) | 65.8 (46-84) | 65.8 (46-85) |
| CA19-9 median (range) U/mL | 23.0 (1.01-235.1) | 30.0 (3.23-139.5) | 224.8 (0.813-2640) | 357.9 (1.13-1224) | 377.6 (0.813-2878) |

**Table S6.** Demographics of neoadjuvant treated pancreatic cancer patients.

| | Therapy Patients | |
|---|---|---|
| | Good/partial response | Poor response |
| Sex (No. of Patients) | | |
| Men No. (%) | 7 (52.1) | 8 (58.3) |
| Women No. (%) | 6 (47.9) | 2 (41.7) |
| Age median (range) year | 61.9 (41-74) | 62.0 (48-73) |
| Cancer stage | | |
| Stage I No. (%) | 3 (23) | 0 (0) |
| Stage II No. (%) | 10 (77) | 10 (100) |

References


1. Logsdon, C.D., *et al.* Molecular profiling of pancreatic adenocarcinoma and chronic pancreatitis identifies multiple genes differentially regulated in pancreatic cancer. *Cancer Res.* **63**, 2649-2657 (2003).
2. Pei, H., *et al.* FKBP51 affects cancer cell response to chemotherapy by negatively regulating Akt. *Cancer Cell* **16**, 259-266 (2009).